Hydrogen bond-stabilized mixtures for efficient carbon dioxide capture

Journal of CO2 Utilization 102 (2025) 103249

Contents lists available at ScienceDirect

Journal of CO2 Utilization

journal homepage: www.elsevier.com/locate/jcou

Hydrogen bond-stabilized mixtures for efficient carbon dioxide capture

Joaquín Arata Badano [a,b,1], Giuseppe Ferraro [c], Daniele Motta [b], Claudia Barolo [b,d], Sergio Bocchini [c], Jorge Gustavo Uranga [a,*], Matteo Bonomo [b,e,**]

[a] Instituto de Investigaciones en Físico-Química Córdoba, Universidad Nacional de Córdoba (INFIQC-CONICET), Córdoba 5000, Argentina
[b] Department of Chemistry, NIS and INSTM Reference Centre, Università di Torino, Via P. Giuria 7, 10125 and Via G. Quarello 15/A, Torino 10135, Italy
[c] Department of Applied Science and Technology, Politecnico di Torino, Corso Duca degli Abruzzi 24, Turin 10129, Italy
[d] Institute of Science, Technology and Sustainability for Ceramics (ISSMC-CNR), Via Granarolo 64, Faenza 48018, Italy
[e] Department of Basic and Applied Science for Engineering, La Sapienza, University of Rome, Via del Castro Laurenziano 7, Rome 00161, Italy

ARTICLE INFO

Keywords:
Carbon capture
Amine-based absorbents
Hydrogen bonding
Solvent stability

ABSTRACT

In this study, we investigate the use of hydrogen bond-stabilized amine-based mixtures (a class of systems hereafter referred to as Hydrogen Bond-Stabilized Mixtures, HBSMs; e.g., n-butylamine with glycerol or guanidinium chloride) as an alternative approach to improve carbon dioxide capture efficiency while avoiding massive solvent evaporation. CO_2 capture experiments reveal that these mixtures exhibit improved sorption capacity compared to pure amines, while the presence of hydrogen bond acceptors plays a crucial role in stabilizing the systems, due to the establishment of an extended hydrogen-bond network. ATR-IR analyses confirm that CO_2 capture occurs through a combination of physical and chemical absorption; on the other hand, TGA data reveal a substantial reduction in solvent evaporation rates, particularly in the n-butylamine/glycerol mixture, where evaporation decreased by more than an order of magnitude compared to pure amine. The high CO_2 absorption capacity and reduced amine volatility of these mixtures open a promising avenue for more sustainable and energy-efficient carbon capture technologies, paving the way for relevant industrial applications.

1. Introduction

Since the industrial revolution, the Earth's average temperature has been steadily increasing due to the rising concentration of greenhouse gases (GHGs) in the atmosphere. This increase is primarily driven by the burning of fossil fuels for energy production, which releases different heat-trapping gasses, especially carbon dioxide (CO_2) [1,2]. Albeit the use of energy is ineluctable in modern society, the related environmental issues are increasingly urgent and problematic [3]. In this context, the widespread use of renewable energy sources, which do not emit any GHGs in the production phase, could be a valuable strategy to reduce emissions; however, the dependence on fossil fuels and the associated emissions will remain a dramatic issue in the near future. Aiming at mitigating this problem, significant scientific efforts have been directed towards the reduction of atmospheric CO_2 concentrations. In this scenario, Carbon Capture, Utilization, and Storage (CCUS) technologies have emerged as a promising solution for avoiding the carbon dioxide release in the atmosphere and promoting its conversion into fuels or other valuable chemicals [4,5].

Recently, several technologies, including absorption, adsorption, cryogenic methods, and membrane technologies, have been employed to capture CO_2, each offering unique benefits and facing distinct challenges [6]. Adsorption methods, which usually employ porous solid materials, present several advantages over liquid absorbents. These include high resistance to material loss, negligible volume changes during operation, resistance to elevated temperatures, and reduced corrosive effects [7]. However, high operating and regeneration costs limit the exploitation of these systems, since the adsorption mechanism is restricted to the exposed material's surface, which requires periodical regeneration [8,9]. On the other hand, cryogenic methods represent a clean technology capable of high-purity CO_2 capturing. These processes involve compression, expansion, separation, and cooling, which, while effective, lead to significant operational costs and a strong dependence on maintaining specific temperature conditions. The latter, combined with the

* Corresponding author.
** Corresponding author at: Department of Basic and Applied Science for Engineering, La Sapienza, University of Rome, Via del Castro Laurenziano 7, Rome 00161, Italy.
E-mail addresses: jorge.uranga@unc.edu.ar (J.G. Uranga), matteo.bonomo@uniroma1.it (M. Bonomo).
[1] Currently at Department of Chemical Science and Technologies, University of Rome Tor Vergata, Via della Ricerca Scientifica 1, 00133 Rome, Italy.

https://doi.org/10.1016/j.jcou.2025.103249
Received 21 July 2025; Received in revised form 4 October 2025; Accepted 13 October 2025
Available online 17 October 2025

stringent control of impurity levels, constrains the feasibility of large-scale implementation of the technology [10,11]. In recent years, membrane technologies, which can be classified into inorganic, organic, and hybrid systems, have gained attention for their low energy consumption, operational simplicity, minimal environmental impact, and compatibility with other CO_2 capture processes. Despite these advantages, membranes face critical challenges, including high initial costs, low selectivity, time-consuming procedures, and limited lifespans, which have hindered their widespread adoption on the industrial scale [12]. In the above discussed scenario, absorption processes, which can be divided into physical and chemical, remain among the most extensively studied and applied methods for CO_2 capture. Physical absorption relies simply on the interaction of carbon dioxide with solvents through weak van der Waals forces, without involving any chemical reactions. This process is typically conducted at high pressures to obtain acceptable carbon dioxide capture values, with solvent regeneration achieved by slightly increasing the temperature and/or by decreasing pressure. As such, physical methods offers limited CO_2 uptake but an extremely easy solvent regeneration and CO_2 release. However, one should note that the solvents used in physical absorption often exhibit low vapor pressure, toxicity, and corrosiveness, and therefore their application is restricted mainly due to safety concerns [13]. In contrast, chemical absorption involves an actual chemical fixation of CO_2 which reacts with specific functional groups available in the solvent to form (weak-to-strong) bound intermediates, for which the release of CO_2 is quite trickier requiring relatively high temperatures and longer regeneration times. Among these solvents, amine-based absorbents, such as aqueous alkanolamine solutions and especially monoethanolamine (MEA), have gained significant attention due to their high reactivity with CO_2, low cost, wide availability, and low viscosity [14]. The high efficiency and economic viability of chemical absorption has established its position as the dominant approach for large-scale CO_2 capture technologies [15]. However, the use of amine-based solvents is limited by several challenges that still must be addressed, including high volatility, toxicity, degradation, corrosion, high energy demand for regeneration and the release of harmful byproducts (*e.g.* nitrosamines) into the environment [16].

To address these challenges, alternative solvents have been investigated which couple suitable physicochemical properties and easiness in recycling and reuse [17,18]. Greener solvents, such as ionic liquids (ILs), deep eutectic solvents (DESs), and liquid polymers (LPs), have been reported for CO_2 absorption via both physical and chemical mechanisms [19]. ILs, organic salts whose melting temperature is lower than their decomposition temperature [20], have been extensively investigated for CO_2 capture due to their unique properties, including negligible vapor pressure, which reduces the energy required for solvent regeneration and CO_2 stripping, excellent thermal and chemical stability, non-corrosive and non-flammable nature, and tunable chemistry through cation and anion engineering [18]. Numerous studies have demonstrated carbon dioxide capture using room-temperature ILs; however, their absorption efficiencies are generally limited due to the high viscosity of the solvent [21]. Furthermore, the high cost and complexity of IL preparation, along with uncertainties regarding their environmental toxicity, make their large-scale industrial application unpredictable [15].

More recently, DESs emerged as a more sustainable alternative to ILs, being characterized by the exploitation of more environmentally friendly, ease to synthesize and low cost precursors, resulting in a less toxic and more biodegradable solution [22,23]. As an added value, DESs can be obtained from natural sources and avoid the use of moisture-free and oxygen-free atmosphere while showing less energy-demanding solvent regeneration after CO_2 uptake, paving their exploitation as carbon dioxide sponges. From a chemical perspective, DESs are eutectic mixtures of Lewis or Brønsted acids and bases containing a range of either anionic and cationic species which can act as hydrogen bond acceptor (HBA) or hydrogen bond donor (HBD) [17]. HBDs include, among others, amides, thioureas, amines, imidazole, azoles, alcohols, acids, whereas the most common HBAs are based on quaternary ammonium salts, imidazole salts, inorganic salt (hydrated or not) and amino acids (AA) [24,25].

Additionally, different amine-functionalized solvents have been reported as efficient systems for CO_2 capture. The enhanced performance of these mixtures has been explained by the presence of amino moieties, which allow specific interactions with carbon dioxide and enhance its effective sorption within the mixture; indeed, extensive reviews on CO_2 capture with ionic liquids and related amine-based systems have also highlighted the key role of hydrogen bonding and molecular interactions in dictating capture efficiency and reversibility [26,27]. Choline chloride—AA based mixtures have demonstrated their potential as sustainable alternatives for CO_2 capture, retaining efficiency over multiple absorption-desorption cycles, with the desorption process occurring at lower temperatures than those required for traditional amine solutions [28,29]. It has also been demonstrated that the capture mechanism is affected by the operating conditions: at low pressure, chemical sorption occurs via carboxylation of the AA anion, whereas at higher pressure, enhanced CO_2 uptake is driven by physical sorption. [30]. Similar findings were also reported for tetraalkylammonium-lysine ILs, exhibiting reversible CO_2 absorption and desorption behavior [21, 31]. Further investigations on the use of choline chloride-amine mixtures confirmed the chemisorption of CO_2, resulting in carbamate formation [32–34]. Furtado *et al.* prepared triethylamine-glycerol mixtures and demonstrated that tertiary amines can act as a base, promoting the formation of an organic carbonate, instead of directly react with CO_2 to form carbamates, positively influencing the reversibility of the process [35]. A similar trend was also reported for MEA-imidazole-ethylene glycol (EG) mixture. The results indicate that CO_2 not only binds with the amino group of MEA to form a carbamate but also reacts with EG (deprotonated by imidazole) leading to the formation of carbonates [36].

Despite significant advancements in amine-based CO_2 capture technologies, challenges such as high regeneration energy requirements, volatility, degradation, and operational costs continue to hinder large-scale applications. Volatility, in particular, remains a critical issue, leading to solvent losses through evaporation during operation, which reduces process efficiency while raising safety and environmental concerns due to the release of volatile organic compounds and potentially toxic byproducts. As such, mitigating volatility is essential to enhance the sustainability, cost-effectiveness, and industrial scalability of these systems. In this regard, the development of non-volatile amine solvents (NVAS), in which the amine is stabilized by extensive inter and intramolecular interaction has recently emerged as a promising approach to overcome volatility limitations while maintaining high CO_2 sorption efficiency [34,37].

Throughout this study, amine-based mixtures were prepared by combining n-butylamine with glycerol or guanidinium hydrochloride to assess the role of these compounds in enhancing CO_2 capture and reducing amine evaporation. The CO_2 capture capacity was determined using a gravimetric method, while absorption/desorption behavior was monitored through *in operando* ATR-IR spectroscopy. The thermal properties of the mixtures were analyzed using thermogravimetric analysis (TGA) and differential scanning calorimetry (DSC), and the evaporation rate was measured gravimetrically using the same setup as the gravimetric absorption experiments.

2. Materials and methods

2.1. Materials

Choline chloride (ChCl) ≥ 99 % (CAS 67–48–1), guanidinium chloride (GuaHCl) ≥ 99 % (CAS 50–01–1), n-butylamine ($ButNH_2$) ≥ 99 % (CAS 109–73–9) and glycerol (Gly) ≥ 99 % (CAS 56–81–5) were purchased from Merck Company. CO_2 4.7 and nitrogen (N_2) 5.0 were

Table 1
Composition of the absorbent solvents tested throughout this work.

Mixture	$ButylNH_2$	Gly	GuaHCl/ Gly	ChCl/ Gly	GuaHCl/ $ButylNH_2$	$ButylNH_2$/ Gly
Molar ratio	-	-	1:2	1:3	1:2	1:2

supplied from Nippon Gases.

2.2. Synthesis of glycerol-based mixtures

Previously dried ChCl, GuaHCl, $ButNH_2$ and Gly were added into a 25 ml flask to prepare mixtures with specific ratios as summarized in Table 1. The mixtures were stirred using a magnetic bar in a double-neck flask at 60 °C under nitrogen atmosphere until a homogeneous liquid phase was obtained. Higher temperatures were avoided to prevent any possible sample degradation. The molar ratios employed were selected as representative stoichiometries to explore possible hydrogen-bonded networks. Although the choice was not the result of a systematic optimization, these ratios reproducibly yielded homogeneous liquids at room temperature and therefore were adopted as model systems for this study.

2.3. Solvent mixture characterization

2.3.1. Proton nuclear magnetic resonance

Proton nuclear magnetic spectra (^{1}H NMR) were acquired at room temperature using a spectrometer (Bruker, Avance 600 MHz, Germany). The samples were placed in 5 mm NMR glass tubes and dimethyl sulfoxide (DMSO-d6), used as solvent and internal reference. Peak identification and spectral processing were carried out using MestReNova software.

2.3.2. Attenuated total reflection infrared spectroscopy

Attenuated total reflection Fourier transformed infrared spectroscopy (ATR-FTIR) was employed to characterize the mixtures and to evaluate their interaction with CO_2. The infrared spectra were recorded using a Bruker Tensor II Fourier transform spectrophotometer (Billerica, MA, USA). A drop of liquid was analyzed using ATR mode equipped with a mercury-cadmium-telluride (MCT) cryogenic detector. The spectra were acquired by accumulating the 32 scans (64 for the background spectrum) in the 4000–500 cm^{-1} range with a resolution of 2 cm^{-1}.

2.3.3. Thermogravimetric-coupled infrared absorption analyses

Thermogravimetric-coupled infrared absorption analyses (TGA-IR) were carried out in a thermogravimetric analyzer NETZSCH TG 209 F1 coupled by a transfer line heated at 230 °C with an infrared spectrometer Bruker TENSOR II equipped with an IR gas cell heated at 200 °C. The tests were performed by heating samples of about 3 mg in alumina pans from 30 °C to 800 °C with a rate of 20 °C min^{-1}, under nitrogen flux of 40 ml min^{-1}. The FTIR data were collected in the absorbance mode in the range 4400–600 cm^{-1}. The first derivative of the weight profile (DTG) was calculated to better resolve the main thermal decomposition steps of the analyzed materials with Netzsch Proteus Analysis software.

2.3.4. Differential scanning calorimetry

Differential scanning calorimetry (DSC) was carried out employing a Netzsch DSC 204 F1 Phoenix in the temperature range from −70 °C to 150 °C at a heating/cooling rate of 20 °C min^{-1} under nitrogen flux. A heat–cool–heat procedure was performed, and the glass transition temperature (T_g) was taken at the inflexion point (if present) of the glass transition step in the third (heating) cycle. The data obtained were processed with Netzsch Proteus Analysis software. Additionally, the melting point (T_m) of the samples in $ButNH_2$-based mixtures was also determined using a manual thermometer-based method [38]. Each mixture was initially frozen by immersing the vial in a Dewar flask containing liquid nitrogen (−196 °C), utilizing headspace cooling to avoid direct contact with the nitrogen. After freezing, by keeping the temperature at −80 °C for 15 min, the mixture was allowed to warm gradually to room temperature. The T_m was recorded as the temperature indicated by the thermometer at the moment of its removal from the vial, ensuring no solid residues were present on its surface. Each measurement was repeated three times to ensure reproducibility.

2.4. Quantification of carbon dioxide absorption

The CO_2 absorption was quantified using a gravimetric method.

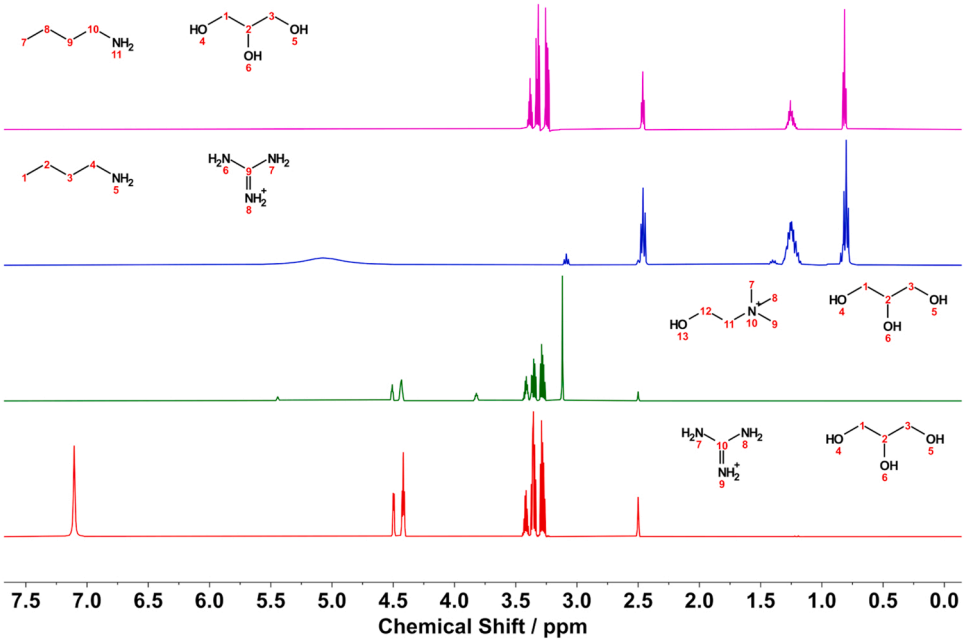

Fig. 1. ^{1}H NMR spectra of (from bottom to top) GuaHCl/Gly (1:2) (red), ChCl/Gly (1:3) (green), GuaHCl/$ButylNH_2$ (1:2) (blue) and $ButylNH_2$/Gly (1:2) (magenta). Chloride anion is omitted for clarity.

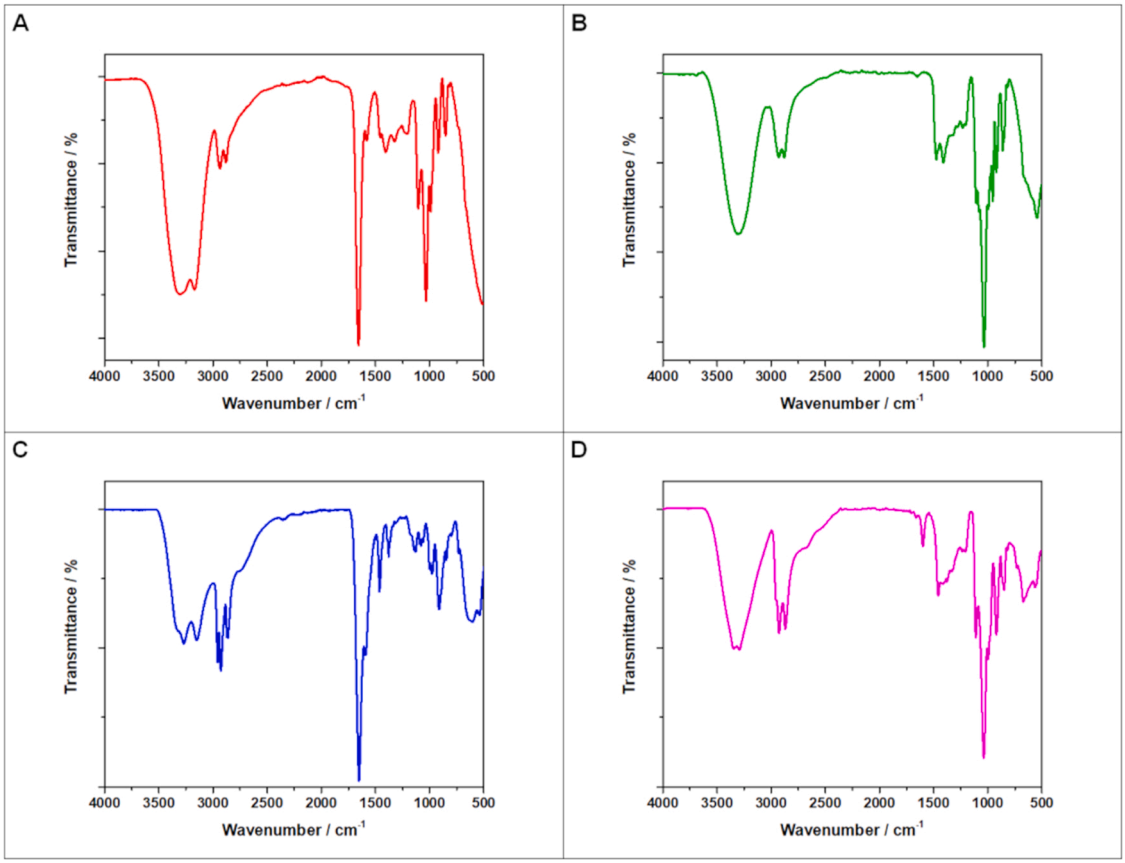

Fig. 2. ATR-FTIR spectra of A) GuaHCl/Gly (1:2) (red), B) ChCl/Gly (1:3) (green), C) GuaHCl/ButylNH2 (1:2) (blue) and D) ButylNH2/Gly (1:2) (magenta).

Approximately 1.5 ml of sample was poured into a batch reactor (~ 4.5 ml), purged for 10 min under nitrogen flux (20 ml min^{-1}) and weighed. Then, the CO_2 (20 ml min^{-1}) was bubbled at room temperature (25 ± 2 °C, 1 atm) until no mass increase was observed. During the whole procedure, the solution was kept under stirring. The captured CO_2 was calculated by mass difference before and after CO_2 contact, considering the reactor headspace contribution.

2.5. Assessment of absorption/desorption and evaporation effect

At the end of the absorption process, a portion of each mixture was sampled to perform a comparative ATR-FTIR analysis. The remaining portion was then heated up to 50 °C for 30 min while bubbling nitrogen through it, aiming to evaluate the reversibility of the CO_2 uptake. To evaluate solvent evaporation under gas flow, the same setup used for gravimetric absorption experiments was employed, with nitrogen as the sole carrier gas. Mass loss was monitored by weighting the reactor containing the solvent sample at one-minute intervals to accurately track the decrease in sample mass over time.

3. Results and discussion

3.1. Solvent mixture characterization

3.1.1. Proton nuclear magnetic resonance

The component ratio of the mixture was confirmed by ^{1}H NMR spectroscopy (Fig. 1): [GuaHCl][Gly] (600 MHz, DMSO-d6): 3.29 (p, 4 H, CH_2), 3.36 (p, 4 H, CH_2), 3.41 (p, 2 H, CH), 4.42 (t, 4 H, OH), 4.50 (dd, 2 H, OH), 7.10 (s, 6 H, NH_2). [ChCl][Gly] (600 MHz, DMSO-d6): 3.12 (t, 9 H, CH_3), 3.29 (p, 6 H, CH_2), 3.35 (p, 6 H, CH_2), 3.41 (m, 5 H, CH, CH_2), 3.82 (m, 2 H, CH_2), 4.42 (t, 6 H, OH), 4.50 (dd, 3 H, OH), 5.44 (t, 1 H, OH). [GuaHCl][$ButNH_2$] (600 MHz, DMSO-d6): 0.80 (t, 6 H, CH_3), 1.25 (m, 8 H, CH_2), 2.46 (t, 4 H, CH_2), 5.07 (s, 10 H, NH_2). [$ButNH_2$][Gly] (600 MHz, DMSO-d6): 0.81 (t, 3 H, CH_3), 1.26 (m, 4 H, CH_2), 2.46 (t, 2 H, CH_2), 3.26 (q, 4 H, CH_2), 3.32 (q, 4 H, CH_2), 3.38 (p, 2 H, CH). Here, it is important to recall, as meaningful absence, the absence of the peak of water (at 3.33 ppm) in all the mixtures as the residual presence of water molecules would alter the hydrogen bond network, impacting on the CO_2 capture ability of the mixtures.

3.1.2. Infrared characterization of mixtures

Pure GuaHCl/Gly (1:2), ChCl/Gly (1:3), GuaHCl/$ButylNH_2$ (1:2) and $ButylNH_2$/Gly (1:2) have been preliminary characterized by ATR-FTIR spectroscopy (Fig. 2), aiming to prove the successful synthesis of the solvents and to unequivocally identify the main spectral features that will be involved in the CO_2 absorption process.

In Fig. 2A the ATR-FTIR spectrum for GuaHCl/Gly (1:2) is presented. The broad peak at 3300 cm^{-1} is assigned as O—H stretching vibration of Gly while the partially overlapped peak at 3170 cm^{-1} is attributed to N—H stretching vibration existing in the GuaHCl [25,39]. Peaks barely visible at 2940 and 2880 cm^{-1} can be ascribed to the asymmetric and symmetric C—H stretching vibrations [40]. The strong signal at 1655 cm^{-1} was assigned to the N—H bending vibrations of GuaHCl [41]. Gly was also identified due to the presence of the typical fingerprint peaks between 852 and 1105 cm^{-1} [42–44]. The peaks at 852 and 921 cm^{-1} are ascribable to the C—C vibrations of the skeleton. Nonetheless, certain studies [25,36] have erroneously attributed the peak around 990 cm^{-1} to the same vibrational mode. Actually, the feature at 990 cm^{-1}, along with the peak detectable at 1033 cm^{-1}, should be imputed to the C—O stretching vibrations in -CH_2OH group, which gives rise to two distinct peaks due to the prochiral nature of the molecule [45]. The C—O stretching associated with the -CHOH moiety is instead observed at 1105 cm^{-1}. Similar peaks can be identified for ChCl/Gly (1:3) (Fig. 2B). The broad peak at 3300 cm^{-1} can be assigned to O—H

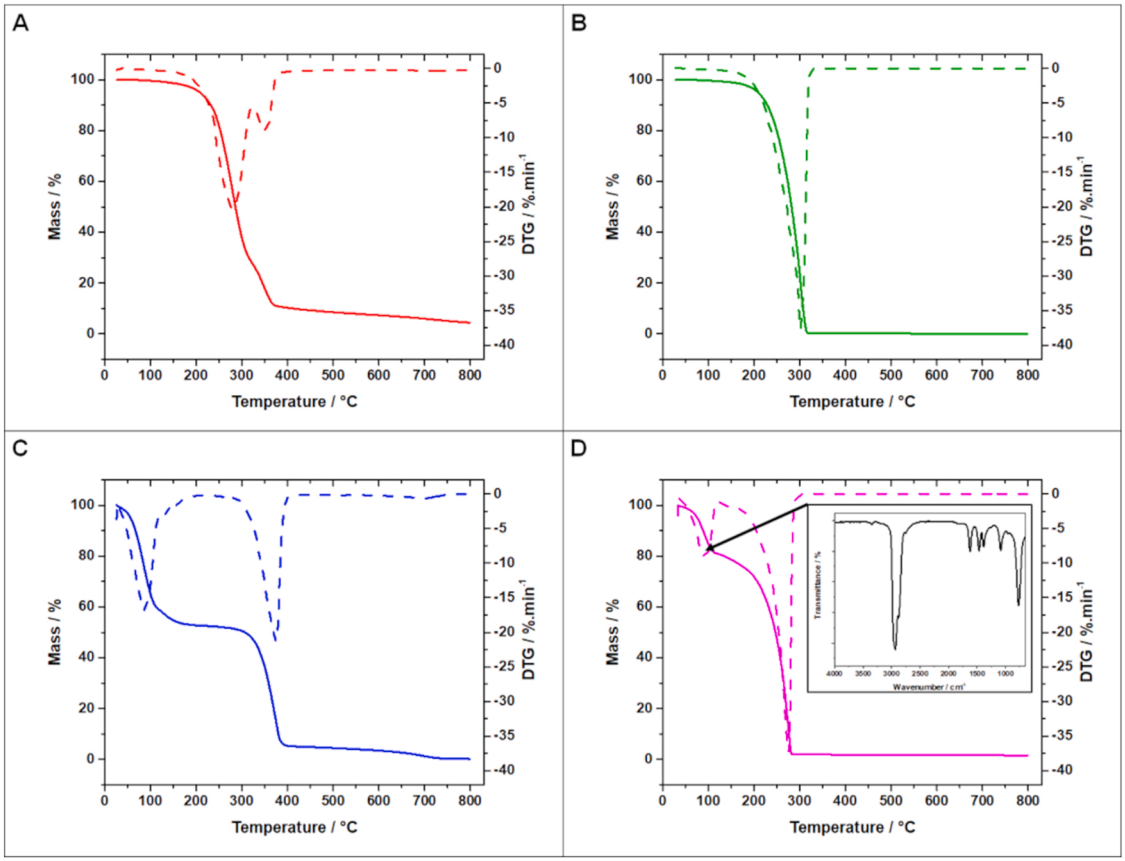

Fig. 3. TGA and DTG thermograms of A) GuaHCl/Gly (1:2), B) ChCl/Gly (1:3), C) GuaHCl/ButylNH$_2$ (1:2) and D) ButylNH$_2$/Gly (1:2). Inset of D: IR spectra of ButylNH$_2$/Gly (1:2) gases after heating up to 94 °C.

stretching vibration, whereas those at 2930 and 2880 cm^{-1} can be attributed to the asymmetric and symmetric C—H stretching vibrations, respectively, of both ChCl and Gly. The bands at 1480–1410 cm^{-1} refer to C—H bending of methylene and methyl groups. Also, the signals corresponding to C—C and C—O stretching vibrations were clearly identified. Fig. 2C shows the spectrum of GuaHCl/ButylNH$_2$ (1:2). The peaks at 3270 and 3150 cm^{-1} are attributed to N—H stretching vibration of ButNH$_2$ and GuaHCl, respectively. A broad overlapped peak at 3300 cm^{-1} is assigned as O—H stretching vibration. Several peaks between 2960 and 2860 cm^{-1} are assigned to the asymmetric and symmetric C—H stretching vibrations of methylene and methyl groups of both components. A strong signal visible at 1652 cm^{-1} and a partially overlapped one at 1592 cm^{-1} correspond to the N—H bending vibration of GuaHCl and ButNH$_2$, respectively. A signal corresponding to C—H bending vibrations of methylene and methyl groups are detected at 1464 and 1378 cm^{-1}. The ButylNH$_2$/Gly (1:2) spectrum (Fig. 2D) shows a broad peak at 3300 cm^{-1} assigned to O—H stretching vibration of Gly overlapping with a peak at 3295 cm^{-1} attributed to N—H stretching vibration of the ButNH$_2$. Also, peaks at 2930 and 2870 cm^{-1}, attributed to the asymmetric and symmetric C—H stretching vibrations of methylene and methyl groups can be noticed. A signal at 1600 cm^{-1} can be assigned to N—H bending vibrations of the amine. At 1456 cm^{-1} a signal corresponding to C—H bending vibrations of methylene is shown. The peaks at 848 and 922 cm^{-1} are assigned to C—C vibrations of Gly, while the C—O stretching vibrations corresponding to Gly molecules were detected at 997, 1037 and 1111 cm^{-1}.

3.1.3. *Thermogravimetric analyses*

Thermal gravimetric analysis (TGA) and its first derivative of the weight profile (DTG) were exploited to evaluate the thermal stability of all the examined mixtures (Fig. 3). GuaHCl/Gly (1:2) profile (Fig. 3A) shows two different mass loss steps, the first one corresponds to the degradation of the glycerol which leads to a residual mass around 35 % whereas the one at higher temperatures is ascribable to the thermal decomposition of GuaHCl. On the contrary, profile in Fig. 3B shows only one mass loss step pointing toward a concurrent thermal degradation of both HBA and HBD, at least in our experimental condition, in good agreement with that previously reported on DESs containing ChCl and Gly [40,46].

On the other hand, ButylNH$_2$-based mixtures (Fig. 3C and 3D) are scarcely studied so far and, as far as we are aware, no reports of thermal stability exist. Both GuaHCl/ButylNH$_2$ (1:2) and ButylNH$_2$/Gly (1:2) profiles present two main mass loss steps, the first one ascribable to amine evaporation and the latter one to the thermal degradation of the parent component. Quite interestingly, the formation of the mixtures leads to a stabilization of the amine compared to the pure amine which is extremely volatile making the recording of its TGA profile quite unreliable. Having a closer look at the TGA profiles, one can note that both the mixtures show a first plateau at higher %mass than expected (45 % vs 37 % and 79 % vs 71 % for GuaHCl/ButylNH$_2$ (1:2) and ButylNH$_2$/Gly (1:2), respectively), this suggesting a good stabilization of a portion (27 % and 13 %, respectively) of ButylNH$_2$ within the mixture, following on from the establishment of an extended hydrogen bond network. In other words, mixtures with strong HB interactions are more resilient to thermal degradation [32]. Such evidence leads to a widening of the temperature range to be exploited for CO_2 adsorption process, making the designed mixtures suitable for implementation in industrial applications, such as CO_2 capture in both pre-combustion and post-combustion stages. The loss of ButNH$_2$ in the ButNH$_2$/Gly (1:2) mixture was confirmed by TGA coupled with infrared spectroscopy. The IR spectra of the evolved gases upon heating up to 94 °C indicate the evaporation of the amine, as evidenced by the presence of characteristic

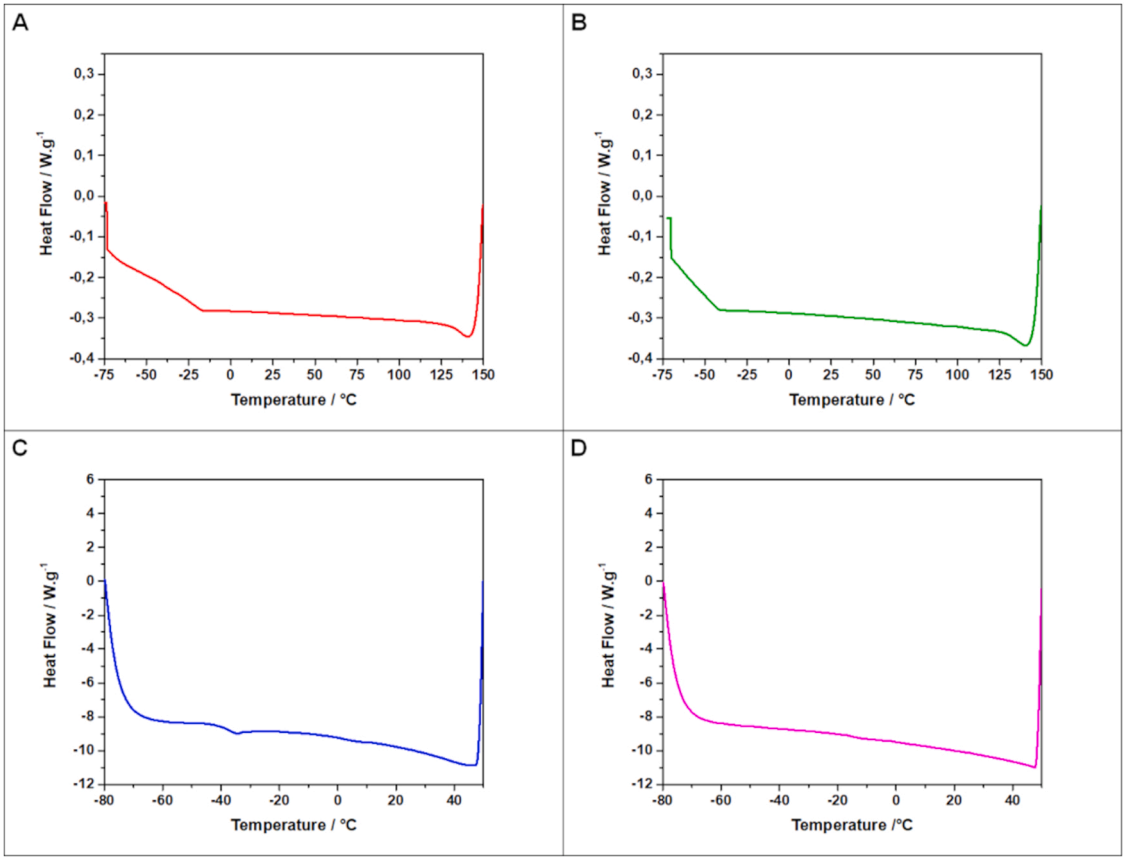

Fig. 4. DSC curves (exothermic up) of A) GuaHCl/Gly (1:2), B) ChCl/Gly (1:3), C) GuaHCl/ButylNH$_2$ (1:2) and D) ButylNH$_2$/Gly (1:2).

bands, including N—H stretching and bending vibrations, as well as C—H stretching and bending modes, consistent with those previously discussed in Section 3.1.2. These results indicate a 20 wt% loss of amine from the mixture, resulting in a more stable composition with an effective amine-to-glycerol ratio of 1:6.

3.1.4. *Differential scanning calorimetry*

The thermal properties of prepared mixtures were evaluated by DSC as shown in Fig. 4, with a particular focus on their DES-like behavior. The recorded thermograms show no changes in the slope of the curves or in the endo/exothermic peaks were observed, indicating that the solvent does not exhibit either a glass transition or a phase change within the selected temperature range suggesting that the mixture kept their fluid state even at extremely low temperature (-70 °C) and they could be preliminary classified as DESs. Data collected for ChCl/Gly (1:3) are in agreement with the literature [47]; on the other hand, to the best of our knowledge, the DSC profiles of the other mixtures have never been reported. Beyond the absence of resolvable transitions at 20 °C min^{-1} , the DSC baselines indicate a distinctly higher apparent heat capacity for the ButylNH$_2$-containing mixtures (GuaHCl/ButylNH$_2$, 1:2; ButylNH$_2$/Gly, 1:2) compared with the salt–glycerol systems (GuaHCl/Gly, 1:2; ChCl/Gly, 1:3). This trend is qualitatively consistent with low-melting, non-ionic liquids. In addition, very weak inflections are visible around −35 °C for GuaHCl/ButylNH$_2$ and around −5 °C for ButylNH$_2$/Gly (Fig. 4C–D), which we tentatively ascribe to subtle phase consolidation (*e.g.* two-phase to one-phase) or micro-reorganization rather than true thermodynamic transitions,. However, aiming at a fairer estimation of the melting temperature of the mixtures, we used an in-house approach (validated in a precedent paper [38]) based on the freezing of the latter at the liquid nitrogen temperature at their slow heating (see experimental section for further details): GuaHCl/ButylNH2 (1:2) and ButylNH2/Gly (1:2) shows a melting temperature of −55 °C and −49 °C, respectively. The latter results are very interesting: on the one hand, the almost null variation of the melting point of GuaHCl/ButylNH2 (1:2) compared to pure ButylNH2 questions the classification of the mixture as a DES (which could be better described as a DES-like system) and to the quantitative replacement of ButylNH2-ButylNH2 interaction with GuaHCl-ButylNH2 with both the components play the double role of HBD and HBA [34,48]. On the other hand, the significant depression of the melting point of Gly (which is the majority component of the GuaHCl/ButylNH2 (1:2) mixture points toward the formation of a DES in which the glycerol and the amine play the role of HBD and HBA, respectively, and characterized by the establishment of a strong and diffuse hydrogen-bond network. Notwithstanding their physical-chemical description, all the mixtures (hereafter generally referred to as hydrogen-bond stabilized mixtures, HBSMs) were tested as adsorbent materials for carbon dioxide.

Table 2
CO_2 capture results for the different mixtures.

Sample	ρ [g/cm^3]	MW [g/mol]	CO_2 Capture [%w/w solvent]	CO_2 Capture [nCO_2/n_{solv}]	CO_2 Capture [nCO_2/$nButNH_2$]
Gly	1.273	92.09	0.04	0.0008	-
ButylNH$_2$	0.700	73.14	20.44	0.34	0.34
GuaHCl/Gly (1:2)	1.310	279.71	0.05	0.0032	-
ChCl/Gly (1:3)	1.196	415.89	0.03	0.0028	-
GuaHCl/ ButylNH$_2$ (1:2)	0.927	241.82	12.33	0.68	0.34
ButylNH$_2$/ Gly (1:2)	1.037	257.32	9.22	0.54	0.54

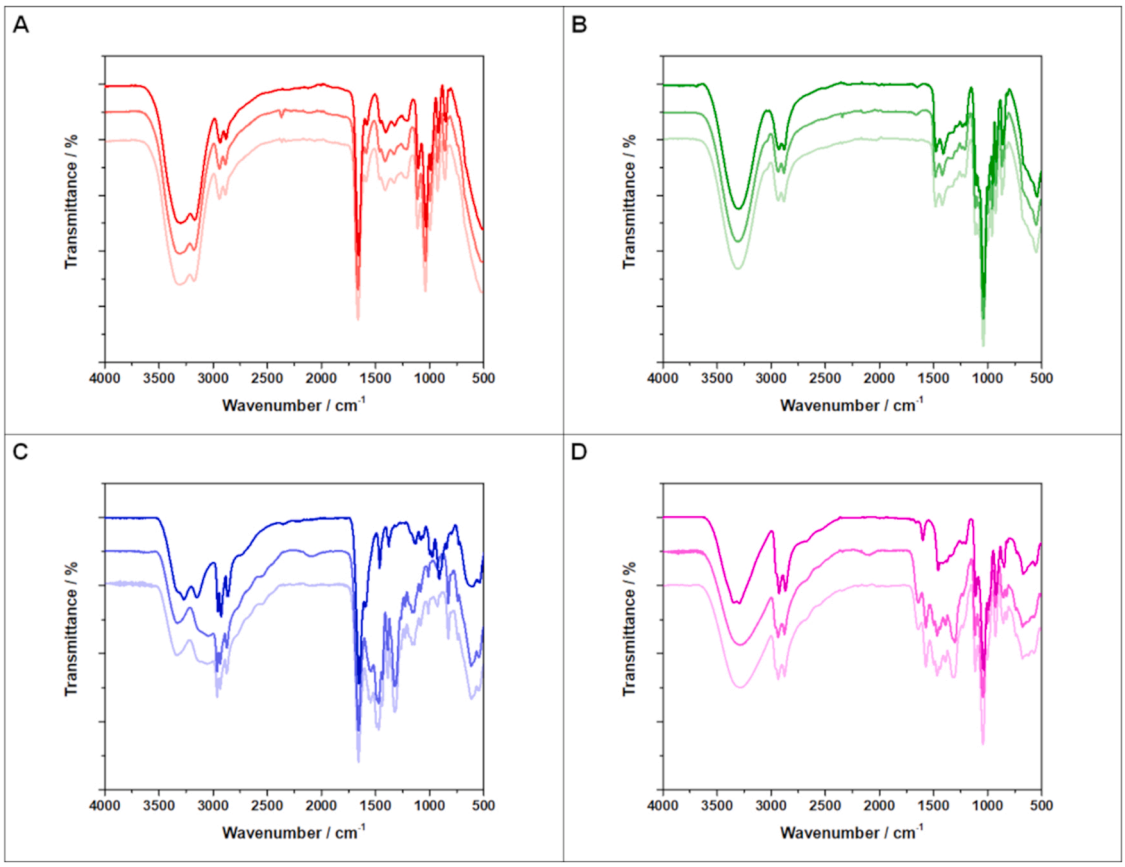

Fig. 5. ATR-FTIR spectra of (A) GuaHCl/Gly (1:2) in shades of red, (B) ChCl/Gly (1:3) in shades of green, (C) GuaHCl/ButylNH$_2$ (1:2) in shades of blue and (D) ButylNH$_2$/Gly (1:2) in shades of magenta. In all cases, the darkest shade represents the pristine solvent, the intermediate shade corresponds to the solvent after CO_2 capture, and the lightest shade indicates the solvent after CO_2 desorption.

3.2. Quantification of carbon dioxide absorption

The absorption capacities (AC) of pure solvents and the different HBSMs were determined and are summarized in Table 2. When pure solvents are analyzed, ButNH$_2$ achieves the highest CO_2 capture in terms of weight percentage (> 20 %w/w), as expected, whereas Gly exhibits a very limited uptake (< 0.05 %w/w). The addition of GuaHCl or ChCl as hydrogen bond acceptors to glycerol has a positive effect on CO_2 capture, leading to a 4-fold increase in the molar uptake. This effect, according to hole theory, could be due to the disruption of strong HBD self-interaction of glycerol which leads to an increase in the free volume of the solvent, allowing more CO_2 to be physically absorbed. This mechanism is driven by van der Waals-type interactions between CO_2 and HBD and HBA of the solvent, allowing a reversible CO_2 absorption without impacting the structural stability of the solvent and suggests a more energy-efficient solvent regeneration [7,17,49]. Similar results were reported for ChCl/Gly mixtures at different molar ratios under different pressure and temperature [15,50]. Despite this, the uptake values are still considerably lower than those of ButNH$_2$. However, as briefly discussed in the introduction, its extremely high evaporation rate (>25 %/min) prevents any industrial application. As is well known, the capturing mechanism of amine based mixtures involves the reaction between two amine groups and CO_2 to form a carbamate as a final stable product [22], where the nucleophilic attack on the carbon atom of CO_2 by one amine is catalyzed by a second amine, acting as a Brønsted base and enabling the proton transfer required for the formation of ion pairs [51,52]. Even in the case of amines, the incorporation of quaternary ammonium salts has been reported to alter intermolecular interactions following on from the increase the free volume in the solvent, decreasing its viscosity and therefore improving the gas diffusivity throughout the DES [33,53]. Here, the addition of GuaHCl to ButNH$_2$ in a 1:2 ratio allows to maintain the molar CO_2 uptake (whereas the %w/w decreases to 12.3 %) aligning with previous studies on amine-based DESs. More interestingly, the addition of GuaHCl likely leads to a complete reorganization of the hydrogen bond network compared to the pure ammine, which results in being highly stabilized in the HBSM, as mirrored by the much lower evaporation rate (*vide infra*). Similarly, even the addition of two equivalents of glycerol is expected to dramatically impact the formation of the hydrogen bond network and to stabilize the amine. The results are quite impressive: when normalized to the moles of ButNH$_2$, the molar CO_2 uptake of the ButylNH$_2$/Gly (1:2) increases from 0.34 (pure ammine) to 0.54, pinpointing a significant role of Gly in the enhancement of ButylNH$_2$ activity, regardless of whether it participates in a chemical reaction or it contributes through physical absorption (*vide infra*).

1.5 ml of sample, CO_2 (20 ml min^{-1}) was bubbled at room temperature.

3.3. Assessment of absorption/desorption and evaporation effect

To further dig into the chemistry of the absorption process, we employed FTIR spectroscopy to focus on the identification of functional groups involved in the interaction with CO_2 molecules and on the eventual reversibility of the process. When ChCl/Gly (1:3) (Fig. 5A) and GuaHCl/Gly (1:2) (Fig. 5B) spectra are analyzed, no discernible changes are observed between the pristine and post-CO_2 samples; only weak bands around 2300 cm^{-1}, corresponding to the symmetric stretching vibrations of dissolved CO_2, are detected [17,54]. These modes disappear after the desorption step, clearly indicating that the capturing mechanism involves physical absorption rather than chemical

Table 3
Evaporation parameters for the different mixtures.

Sample	Evaporation rate / wt% min-1	Vapor pressure / Pa	Time-normalized stripping energy / kJ mol CO_2^{-1} min^{-1}
Gly	-	-	-
$ButNH_2$	27	12400	28.37
GuaHCl/Gly (1:2)	-	-	-
ChCl/Gly (1:3)	-	-	-
GuaHCl/$ButNH_2$ (1:2)	2.60	73	2.73
$ButNH_2$/Gly (1:2)	0.60	24	0.40

absorption, according to the limited uptake discussed above.

On the other hand, a different behavior was observed for butylamine-based HBSMs. In the spectrum of GuaHCl/$ButNH_2$ (1:2) (Fig. 5C) after the CO_2 uptake, a broader band at 1650 cm^{-1} appears resulting from the overlapping of the C═O stretching band of carbamate species and the N—H bending of GuaHCl [33,36]. Also, several overlapped bands appear in the 1510–1600 cm^{-1} range, attributed to overlapping signals from the N—H bending vibration of carbamates, ammonium ions (—NH_3^+), and amine groups of unreacted solvent [28]. Additionally, the presence of bands around 1300 cm^{-1}, corresponding to C—N and C—O stretching vibrations, confirms the formation of a carbamate [53]. To conclude, the almost perfect overlap between the spectrum of the post-CO_2 absorption mixture and the one of the systems after the nitrogen-based desorption step suggests that the chemical absorption of CO_2 through carbamates formation is, as expected, not reversible. A weak but broad band at 2100 cm^{-1} also indicates a certain amount of physiosorbed (*i.e.* dissolved) CO_2 [53], indicating a (limited) contribution of physical mechanisms to CO_2 uptake. Similar bands have been reported in previous studies for other amine-based DESs used in CO_2 capture, further corroborating the identification of these vibrational modes [32,33,36,53,55]. As observed in Fig. 5D, notable differences can be seen between pristine ButylNH_2/Gly (1:2) and the solvent after CO_2 uptake. New bands appear at 1638 cm^{-1}, 1568 cm^{-1}, 1438 cm^{-1} and 1322 cm^{-1} corresponding to the C═O stretching frequency, COO^- asymmetric and symmetric stretching vibration and N – COO^- stretching vibration of carbamate species, respectively [28,36,56]. Additionally, a band at 1495 cm^{-1}, attributed to the symmetric bending mode of the ammonium ion (—NH_3^+) formed by the second amine group after proton abstraction is noted [28]. Broad bands around 1300 cm^{-1}, corresponding to C—N and C—O stretching frequencies, further confirm the formation of carbamate [53]: two bands at 1386 cm^{-1} and 1298 cm^{-1} corresponding to the C–O and RO-COO^- stretching modes of carbonate might indicate its formation [36]. Even in this case, the weak band around 2100 cm^{-1} (asymmetric and symmetric stretching vibrations of dissolved CO_2) is detected. Similar to GuaHCl/$ButNH_2$ (1:2), the spectrum after desorption step shows no variation compared to the post-CO_2 absorption step.

The above discussed results point toward an irreversible, in the tested conditions (*i.e.* 50 °C, 30 min, N_2 bubbling) at least, formation of carbamate following on from the chemisorption of carbon dioxide. Being the carbamate formation ruled by an equilibrium, the modification of process parameters could induce the desorption reaction. However, higher temperatures or longer times are avoided to prevent the possible thermal decomposition of some of the mixtures (see Fig. 3) and the complete evaporation of the pure amine which would prevent any meaningful comparison. This would be a key issue to be solved by means of mixture engineering to enable multiple sorption/desorption cycles and to improve the recyclability of the adsorbent mixtures.

To be applied on an industrial scale, the sorbent should show long-term stability and ease in handling. As discussed in the introduction, amines usually suffer for consistent evaporation even at room temperature (*i.e.* 27 %w/min for pure ButylNH_2). However, the establishment of an extended hydrogen bond network in the HBSMs could play a significant role: indeed, as shown in Table 3, the addition of a quaternary ammonium salt (GuaHCl) or alcohol (Gly) positively impact the evaporation rate of the amine by significantly reducing down to 2.6 %w/min (one order of magnitude) and 0.60 %w/min (almost two orders of magnitude), respectively, in good agreement with previous studies which have reported on the reduced volatility of salts or organic-solvents enriched amines due to the formation of strong intermolecular interactions [57,58]. It is important to note that the volatility of these mixtures is more strongly influenced by the starting materials than ILs, as weaker interactions (hydrogen bond vs electrostatic interaction) make DESs and HBSMs more susceptible to volatility [59]. However, the addition of Gly, in a 1:2 ratio, leads to the formation of a DES which formidably stabilizes the ammine counterparts whose evaporation rate drops to 0.60 %w/min; moreover, due to the almost null vapor tension shown by DESs, the weight loss is likely due to a slight excess of the amine in DES formulation. To more accurately quantify the reduced volatility of the stabilized mixtures, the Langmuir equation [60,61] was employed to determine their vapor pressures:

$$\frac{dm}{dt} = \alpha\sqrt{\frac{M}{2\pi RT}}P$$

where dm/dt is the evaporation rate per unit area (kg s^{-1} m^{-2}), M the molecular mass of the evaporating material (kg mol^{-1}), R the gas constant (8.314 kg m^2 s^{-2} K^{-1} mol^{-1}), T the absolute temperature (K), P the vapor pressure and α the vaporization coefficient. Unlike in vacuum conditions, α cannot be assumed to be equal to 1, as the experiments were conducted under a flowing gas stream (see Materials and Methods). Using the known vapor pressure of pure butylamine (12.4 kPa [62]), the vaporization coefficient was determined to be 0.79 via the Langmuir equation. This value was then used to estimate the effective vapor pressures of the GuaHCl/$ButNH_2$ (1:2) and $ButNH_2$/Gly (1:2) mixtures, resulting 73 Pa and 24 Pa (Table 3), respectively, both two orders of magnitude lower than pure butylamine.

The improved solvent stability and reduced evaporation rates observed in this study represent a significant advancement for potential CO_2 capture applications. This trend is in line with recent reports on NVAS systems, where the reduction of volatility through molecular design (*e.g.*, DES, ILs, or hyperbranched polyamines) has proven essential for enabling practical large-scale implementation [63]. Enhanced stability minimizes solvent losses and improves process efficiency, making these systems more viable for long-term use. To further confirm this, a regenerative energy calculation was performed using the following equation:

$$ESR = 35.72\frac{nButNH2}{nCO2}$$

where E_{SR} is the energy for the solvent regeneration, 35.72 (kJ mol^{-1}) is the heat of vaporization n-butylamine (and so, the energy to regenerate the sorbent) and $nButNH_2/nCO_2$ is a molar ratio obtained from Table 2 [64]. For both pure butylamine and GuaHCl/$ButNH_2$ mixture, the calculated regenerative energy is 105.06 kJ mol^{-1} CO_2. In contrast, the $ButNH_2$/Gly mixture exhibits a significantly lower energy requirement of 66.15 kJ mol^{-1} CO_2, nearly half that of the two counterparts. However, when evaporation rate is also considered, the trend in energy efficiency changes significantly and becomes $ButNH_2$/Gly < GuaHCl/$ButNH_2$ < $ButNH_2$ with time-normalized regenerative energy of 0.40 kJ mol CO_2^{-1} min^{-1}, 2.73 kJ mol CO_2^{-1} min^{-1} and 28.37 kJ mol CO_2^{-1} min^{-1}, respectively (Table 3), clearly showing the energetic (and therefore economic) benefits that would result from employing these mixtures in carbon capture technologies.

While the reduction of amine evaporation is remarkable, the potential increase in viscosity and corresponding decrease in mass transfer

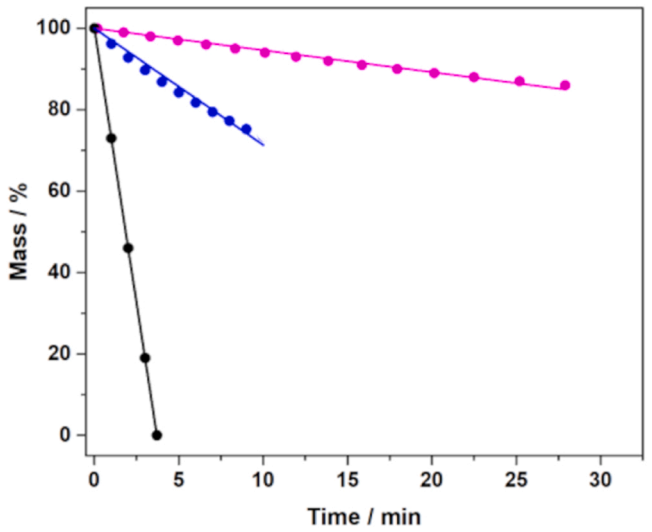

Fig. 6. Evaporation rate for GuaHCl/ButylNH2 (1:2) (blue), ButylNH2/Gly (1:2) (magenta) and ButylNH2 (black).

rates following on from CO_2 uptake must be considered for process scale-up. It is important to recall here that the relatively low amount of solvent used in the uptake tests ensures a high surface-to-volume ratio, minimizing the diffusion issues which could take place in the bulk phase. As such, further HBSM's engineering could be required toward the proposition of our mixtures on a pilot-line scale. Albeit beyond the scope of the present paper, we would like to stress the role of water on a pilot-line scale. Thanks to a thoughtful choice of precursors and mixing process, our mixtures are water-free, but the latter, unavoidable in real gas streams, would alter the hydrogen-bond network, thereby impacting solvent stability and capture efficiency. As such, further mixtures engineering could not overlook the water contributions.

4. Conclusion

In this study, we investigate hydrogen bond-stabilized amine-based mixtures as alternative solvents for efficient CO_2 capture. Our findings demonstrate that the addition of glycerol and guanidinium chloride significantly enhances CO_2 absorption capacity while concurrently mitigating amine volatility. The CO_2 capture experiments, coupled with ATR-IR spectroscopy, confirm that both physical and chemical mechanisms are involved, with the formation of carbamate species playing a crucial role in enhancing absorption efficiency. More interestingly, the incorporation of hydrogen bond acceptors such as glycerol and the consequent formation of an hydrogen bond-stabilized mixture (HBSM) effectively stabilizes n-butylamine, reducing its evaporation rate by almost two orders of magnitude (0.60 w%/min vs 27 w%/min) while maintaining high CO_2 capture efficiency, suggesting their potential for long-term and industrial-scale application. These results highlight the importance of molecular design in optimizing CO_2 capture solvents, offering a more sustainable and energy-efficient alternative to conventional amine-based systems. The demonstrated reduction of volatility, combined with robust CO_2 absorption, positions HBSMs as promising candidates for more sustainable and scalable CO_2 capture technologies. Future studies will further explore the possibility of these mixtures to be exploited in direct air capture applications, also evaluating regeneration efficiency and long-term stability under realistic operating conditions to support their practical application in carbon capture technologies.

CRediT authorship contribution statement

Joaquín Arata Badano: Writing – review & editing, Writing – original draft, Investigation, Formal analysis, Data curation. **Giuseppe Ferraro:** Writing – review & editing, Formal analysis, Data curation. **Daniele Motta:** Writing – review & editing, Visualization, Validation, Data curation. **Barolo Claudia:** Writing – review & editing, Resources, Funding acquisition. **Sergio Bocchini:** Writing – review & editing, Resources, Funding acquisition. **Jorge Gustavo Uranga:** Writing – review & editing, Resources, Project administration, Funding acquisition, Conceptualization. **Matteo Bonomo:** Writing – review & editing, Writing – original draft, Supervision, Resources, Project administration, Methodology, Conceptualization.

Declaration of Competing Interest

The authors declare no conflict of interest.

Acknowledgments

J.A.B, D.M., C.B. and M.B. acknowledge support from Project CH4.0 under the MUR program "Dipartimento di Eccellenza 2023-2027" (CUP D13C22003520001). J.A.B and J.G.U. thank the Argentinian Research Council (CONICET), National University of Córdoba for funding. J.A.B. acknowledge CONICET for financing his postdoctoral fellowship. G.F. received the fund under the Project funded by the European Union – NextGenerationEU under the National Recovery and Resilience Plan (NRRP), Mission 04 Component 2 Investment 3.1 | Project Code IR0000027 – CUP: B33C22000710006 – iEntrance@ENL: Infrastracture for Energy TRAnsition aNd Circular Economy @EuroNano Lab.

Data availability

Data will be made available on request.

References

[1] S. Imteyaz, P.P. Ingole, Comparison of physicochemical properties of choline chloride-based deep eutectic solvents for CO2 capture: progress and outlook, J. Mol. Liq. 376 (2023), https://doi.org/10.1016/j.molliq.2023.121436.
[2] Y. Zhang, X. Ji, X. Lu, Choline-based deep eutectic solvents for CO2 separation: review and thermodynamic analysis, Renew. Sustain. Energy Rev. 97 (2018) 436–455, https://doi.org/10.1016/j.rser.2018.08.007.
[3] M. Chehrazi, B. Kamyab, A review on CO2 capture with chilled ammonia and CO2 utilization in urea plant, J. CO2 Util. 61 (2022) 102030, https://doi.org/10.1016/j.jcou.2022.102030.
[4] M. Aghaie, N. Rezaei, S. Zendehboudi, A systematic review on CO2 capture with ionic liquids: current status and future prospects, Renew. Sustain. Energy Rev. 96 (2018) 502–525, https://doi.org/10.1016/j.rser.2018.07.004.
[5] L. Zhao, H.Y. Hu, A.G. Wu, A.O. Terent'ev, L.N. He, H.R. Li, CO2 capture and in-situ conversion to organic molecules, J. CO2 Util. 82 (2024) 102753, https://doi.org/10.1016/j.jcou.2024.102753.
[6] P. Madejski, K. Chmiel, N. Subramanian, T. Kus, Methods and techniques for CO2 capture: review of potential, Energies 15 (2022) 887.
[7] H. Wibowo, H. Susanto, N. Grisdanurak, D. Hantoko, K. Yoshikawa, H. Qun, M. Yan, Recent developments of deep eutectic solvent as absorbent for co2removal from syngas produced from gasification: current status, challenges, and further research, J. Environ. Chem. Eng. 9 (2021) 105439, https://doi.org/10.1016/j.jece.2021.105439.
[8] G. Leonzio, N. Shah, Recent advancements and challenges in carbon capture, utilization and storage, Curr. Opin. Green. Sustain. Chem. 46 (2024) 100895, https://doi.org/10.1016/j.cogsc.2024.100895.
[9] W.U. Mulk, S.A. Ali, S.N. Shah, M.U.H. Shah, Q.J. Zhang, M. Younas, A. Fatehizadeh, M. Sheikh, M. Rezakazemi, Breaking boundaries in CO2 capture: ionic liquid-based membrane separation for post-combustion applications, J. CO2 Util. 75 (2023) 102555, https://doi.org/10.1016/j.jcou.2023.102555.
[10] L. Fu, Z. Ren, W. Si, Q. Ma, W. Huang, K. Liao, Z. Huang, Y. Wang, J. Li, P. Xu, Research progress on CO2 capture and utilization technology, J. CO2 Util. 66 (2022) 102260, https://doi.org/10.1016/j.jcou.2022.102260.
[11] J.A. Garcia, M. Villen-Guzman, J.M. Rodriguez-Maroto, J.M. Paz-Garcia, Technical analysis of CO2 capture pathways and technologies, J. Environ. Chem. Eng. 10 (2022) 108470, https://doi.org/10.1016/j.jece.2022.108470.
[12] H. Hekmatmehr, A. Esmaeili, M. Pourmahdi, S. Atashrouz, A. Abedi, M. Ali Abuswer, D. Nedeljkovic, M. Latifi, S. Farag, A. Mohaddespour, Carbon capture technologies: a review on technology readiness level, Fuel 363 (2024) 130898, https://doi.org/10.1016/j.fuel.2024.130898.
[13] X.Y.D. Soo, J.J.C. Lee, W.Y. Wu, L. Tao, C. Wang, Q. Zhu, J. Bu, Advancements in CO2 capture by absorption and adsorption: a comprehensive review, J. CO2 Util. 81 (2024) 102727, https://doi.org/10.1016/j.jcou.2024.102727.

[14] M. Kumari, F. Vega, L.M. Gallego Fernández, K. Prasad Shadangi, N. Kumar, Liquid amine functional, aqueous blends and the CO2 absorption capacity: molecular structure, size, interaction parameter and mechanistic aspects, J. Mol. Liq. 384 (2023), https://doi.org/10.1016/j.molliq.2023.122288.
[15] C. Aravena, D. Lee, J. Park, Y. Yoo, Characteristics of deep eutectic solvents for CO2 capture with hydro effects for improvement of mass transfer, J. Ind. Eng. Chem. 111 (2022) 337–345, https://doi.org/10.1016/j.jiec.2022.04.015.
[16] F. Meng, Y. Meng, T. Ju, S. Han, L. Lin, J. Jiang, Research progress of aqueous amine solution for CO2 capture: a review, Renew. Sustain. Energy Rev. 168 (2022) 112902, https://doi.org/10.1016/j.rser.2022.112902.
[17] A. Alnajjar, S.A. Onaizi, CO2 capture and conversion using deep eutectic solvents: recent progress and outlooks, J. Mol. Liq. 421 (2025) 126832, https://doi.org/10.1016/j.molliq.2024.126832.
[18] Y. Xu, R. Zhang, Y. Zhou, D. Hu, C. Ge, W. Fan, B. Chen, Y. Chen, W. Zhang, H. Liu, G. Cui, H. Lu, Tuning ionic liquid-based functional deep eutectic solvents and other functional mixtures for CO2 capture, Chem. Eng. J. 463 (2023) 142298, https://doi.org/10.1016/j.cej.2023.142298.
[19] A. Krishnan, K.P. Gopinath, D.V.N. Vo, R. Malolan, V.M. Nagarajan, J. Arun, Ionic liquids, deep eutectic solvents and liquid polymers as Green solvents in carbon capture technologies: a review, Environ. Chem. Lett. 18 (2020) 2031–2054, https://doi.org/10.1007/s10311-020-01057-y.
[20] A. Mariani, M. Bonomo, X. Gao, B. Centrella, A. Nucara, R. Buscaino, A. Barge, N. Barbero, L. Gontrani, S. Passerini, The unseen evidence of reduced ionicity: the elephant in (the) room temperature ionic liquids, J. Mol. Liq. 324 (2021) 115069, https://doi.org/10.1016/j.molliq.2020.115069.
[21] N. Bera, P. Sardar, R. Hazra, A.N. Samanta, N. Sarkar, Direct air capture of CO2 by amino acid-functionalized ionic liquid-based deep eutectic solvents, ACS Sustain. Chem. Eng. 12 (2024) 14288–14295, https://doi.org/10.1021/acssuschemeng.4c05090.
[22] M.F.H. Ismail, A.N. Masri, N. Mohd Rashid, I.M. Ibrahim, S.A.S. Mohammed, W.Z. N. Yahya, A review of CO2 capture for amine-based deep eutectic solvents, J. Ion. Liq. 4 (2024) 100114, https://doi.org/10.1016/j.jil.2024.100114.
[23] S. Nejrotti, A. Antenucci, C. Pontremoli, L. Gontrani, N. Barbero, M. Carbone, M. Bonomo, Critical assessment of the sustainability of deep eutectic solvents: a case study on six choline Chloride-Based mixtures, ACS Omega 7 (2022) 47449–47461, https://doi.org/10.1021/acsomega.2c06140.
[24] S.E. Hooshmand, S. Kumar, I. Bahadur, T. Singh, R.S. Varma, Deep eutectic solvents as reusable catalysts and promoter for the greener syntheses of small molecules: recent advances, J. Mol. Liq. 371 (2023) 121013, https://doi.org/10.1016/j.molliq.2022.121013.
[25] T. Jurić, D. Uka, B.B. Holló, B. Jović, B. Kordić, B.M. Popović, Comprehensive physicochemical evaluation of choline chloride-based natural deep eutectic solvents, J. Mol. Liq. 343 (2021), https://doi.org/10.1016/j.molliq.2021.116968.
[26] G. Cui, J. Wang, S. Zhang, Active chemisorption sites in functionalized ionic liquids for carbon capture, Chem. Soc. Rev. 45 (2016) 4307–4339, https://doi.org/10.1039/C5CS00462D.
[27] Z. Zhao, K. Wang, H. Tao, Z. Zhang, W. Lin, Q. Xiao, L. Jiang, H. Li, C. Wang, Thermodynamic regulation of carbon dioxide capture by functionalized ionic liquids, Chem. Soc. Rev. 54 (2025) 2091–2126, https://doi.org/10.1039/D4CS00972J.
[28] G. Latini, M. Signorile, V. Crocellà, S. Bocchini, C.F. Pirri, S. Bordiga, Unraveling the CO2 reaction mechanism in bio-based amino-acid ionic liquids by operando ATR-IR spectroscopy, Catal. Today 336 (2019) 148–160, https://doi.org/10.1016/j.cattod.2018.12.050.
[29] G. Latini, M. Signorile, F. Rosso, A. Fin, M. d'Amora, S. Giordani, F. Pirri, V. Crocellà, S. Bordiga, S. Bocchini, Efficient and reversible CO2 capture in bio-based ionic liquids solutions, J. CO2 Util. 55 (2022), https://doi.org/10.1016/j.jcou.2021.101815.
[30] N. Noorani, A. Mehrdad, Experimental and theoretical study of CO2 sorption in biocompatible and biodegradable cholinium-based ionic liquids, Sep. Purif. Technol. 254 (2021) 117609, https://doi.org/10.1016/j.seppur.2020.117609.
[31] S. Saravanamurugan, A.J. Kunov-Kruse, R. Fehrmann, A. Riisager, Amine-functionalized amino acid-based ionic liquids as efficient and high-capacity absorbents for CO2, ChemSusChem 7 (2014) 897–902, https://doi.org/10.1002/cssc.201300691.
[32] S. Sarmad, D. Nikjoo, J.P. Mikkola, Amine functionalized deep eutectic solvent for CO2 capture: measurements and modeling, J. Mol. Liq. 309 (2020) 113159, https://doi.org/10.1016/j.molliq.2020.113159.
[33] D.M. Makarov, M.A. Krestyaninov, A.A. Dyshin, V.A. Golubev, A.M. Kolker, CO2 capture using choline chloride-based eutectic solvents. An experimental and theoretical investigation, J. Mol. Liq. 413 (2024), https://doi.org/10.1016/j.molliq.2024.125910.
[34] J. Gao, X. Yang, Z. Xing, X. Song, Y. Liu, Z. Wang, G. Deng, X. Zhao, Physicochemical and thermodynamic properties of binary amine-based deep eutectic solvents for carbon capture, J. Mol. Liq. 399 (2024) 124346, https://doi.org/10.1016/j.molliq.2024.124346.
[35] I.O. Furtado, T.C. dos Santos, L.F. Vasconcelos, L.T. Costa, R.G. Fiorot, C. M. Ronconi, J.W. de M. Carneiro, Combined theoretical and experimental studies on CO2 capture by amine-activated glycerol, Chem. Eng. J. 408 (2021) 1–8, https://doi.org/10.1016/j.cej.2020.128002.
[36] J. Cheng, C. Wu, W. Gao, H. Li, Y. Ma, S. Liu, D. Yang, CO2 absorption mechanism by the deep eutectic solvents formed by Monoethanolamine-Based protic ionic liquid and ethylene glycol, Int. J. Mol. Sci. 23 (2022), https://doi.org/10.3390/ijms23031893.
[37] J. Gao, Y. Liu, X. Song, S. Wang, Y. Ren, S. Xu, Diluent tailored quaternary deep eutectic solvents for energy efficient carbon capture, Sep. Purif. Technol. 378 (2025) 134623, https://doi.org/10.1016/j.seppur.2025.134623.
[38] F. Cappelluti, A. Mariani, M. Bonomo, A. Damin, L. Bencivenni, S. Passerini, M. Carbone, L. Gontrani, Stepping away from serendipity in deep eutectic solvent formation: prediction from precursors ratio, J. Mol. Liq. 367 (2022) 120443, https://doi.org/10.1016/j.molliq.2022.120443.
[39] Z. Huang, B. Jiang, H. Yang, B. Wang, N. Zhang, H. Dou, G. Wei, Y. Sun, L. Zhang, Investigation of glycerol-derived binary and ternary systems in CO2 capture process, Fuel 210 (2017) 836–843, https://doi.org/10.1016/j.fuel.2017.08.043.
[40] N. Delgado-Mellado, M. Larriba, P. Navarro, V. Rigual, M. Ayuso, J. García, F. Rodríguez, Thermal stability of choline chloride deep eutectic solvents by TGA/FTIR-ATR analysis, J. Mol. Liq. 260 (2018) 37–43, https://doi.org/10.1016/j.molliq.2018.03.076.
[41] Y. Tian, W. Chen, B. Zhang, Y. Chen, R. Shi, S. Liu, Z. Zhang, T. Mu, A weak acidic and strong coordinated deep eutectic solvent for recycling of cathode from spent Lithium-Ion batteries, ChemSusChem 15 (2022) 1–8, https://doi.org/10.1002/cssc.202200524.
[42] Akari Habuka, Takeshi Yamada, Satoru Nakashima, Interactions of glycerol, diglycerol, and water studied using attenuated total reflection infrared spectroscopy, Appl. Spectrosc. 74 (2020) 767–779, https://doi.org/10.1177/0003702820919530.
[43] R. Chelli, F.L. Gervasio, C. Gellini, P. Procacci, G. Cardini, V. Schettino, Density functional calculation of structural and vibrational properties of glycerol, J. Phys. Chem. A 104 (2000) 5351–5357, https://doi.org/10.1021/jp0000883.
[44] M. Sethu Raman, V. Ponnuswamy, P. Kolandaivel, K. Perumal, Ultrasonic and DFT study of intermolecular association through hydrogen bonding in aqueous solutions of glycerol, J. Mol. Liq. 142 (2008) 10–16, https://doi.org/10.1016/j.molliq.2008.03.006.
[45] R. Chelli, P. Procacci, G. Cardini, S. Califano, Glycerol condensed phases part II.A molecular dynamics study of the conformational structure and hydrogen bonding, Phys. Chem. Chem. Phys. 1 (1999) 879–885, https://doi.org/10.1039/A808957D.
[46] A. Mero, S. Koutsoumpos, P. Giannios, I. Stavrakas, K. Moutzouris, A. Mezzetta, L. Guazzelli, Comparison of physicochemical and thermal properties of choline chloride and betaine-based deep eutectic solvents: the influence of hydrogen bond acceptor and hydrogen bond donor nature and their molar ratios, J. Mol. Liq. 377 (2023) 121563, https://doi.org/10.1016/j.molliq.2023.121563.
[47] L. Meredith, A. Elbourne, T.L. Greaves, G. Bryant, S.J. Bryant, Physico-chemical characterisation of glycerol- and ethylene glycol-based deep eutectic solvents, J. Mol. Liq. 394 (2024) 123777, https://doi.org/10.1016/j.molliq.2023.123777.
[48] S.J. Bryant, A.J. Christofferson, T.L. Greaves, C.F. McConville, G. Bryant, A. Elbourne, Bulk and interfacial nanostructure and properties in deep eutectic solvents: current perspectives and future directions, J. Colloid Interface Sci. 608 (2022) 2430–2454, https://doi.org/10.1016/j.jcis.2021.10.163.
[49] B.B. Hansen, S. Spittle, B. Chen, D. Poe, Y. Zhang, J.M. Klein, A. Horton, L. Adhikari, T. Zelovich, B.W. Doherty, B. Gurkan, E.J. Maginn, A. Ragauskas, M. Dadmun, T.A. Zawodzinski, G.A. Baker, M.E. Tuckerman, R.F. Savinell, J. R. Sangoro, Deep eutectic solvents: a review of fundamentals and applications, Chem. Rev. 121 (2021) 1232–1285, https://doi.org/10.1021/acs.chemrev.0c00385.
[50] N. Mirza, K. Mumford, Y. Wu, S. Mazhar, S. Kentish, G. Stevens, Improved eutectic based solvents for capturing carbon dioxide (CO2), Energy Procedia 114 (2017) 827–833, https://doi.org/10.1016/j.egypro.2017.03.1909.
[51] X.E. Hu, Q. Yu, F. Barzagli, C. Li, M. Fan, K.A.M. Gasem, X. Zhang, E. Shiko, M. Tian, X. Luo, Z. Zeng, Y. Liu, R. Zhang, NMR techniques and prediction models for the analysis of species formed in CO2 capture processes with amine-based sorbents: a critical review, ACS Sustain. Chem. Eng. 8 (2020) 6173–6193, https://doi.org/10.1021/acssuschemeng.9b07823.
[52] R.Ben Said, J.M. Kolle, K. Essalah, B. Tangour, A. Sayari, A unified approach to CO2-Amine reaction mechanisms, ACS Omega 5 (2020) 26125–26133, https://doi.org/10.1021/acsomega.0c03727.
[53] J. Ju, D. Choi, S. Cho, Y. Yoo, D. Kang, Absorption characteristics and rheological properties of quaternized polyamine-based deep eutectic solvents for high performance CO2 capture, Chem. Eng. J. 496 (2024) 153922, https://doi.org/10.1016/j.cej.2024.153922.
[54] G. Siani, M. Tiecco, P. Di Profio, S. Guernelli, A. Fontana, M. Ciulla, V. Canale, Physical absorption of CO2 in betaine/carboxylic acid-based natural deep eutectic solvents, J. Mol. Liq. 315 (2020), https://doi.org/10.1016/j.molliq.2020.113708.
[55] H. Ren, S. Lian, X. Wang, Y. Zhang, E. Duan, Exploiting the hydrophilic role of natural deep eutectic solvents for greening CO2 capture, J. Clean. Prod. 193 (2018) 802–810, https://doi.org/10.1016/j.jclepro.2018.05.051.
[56] S. Sarmad, Y. Xie, J.P. Mikkola, X. Ji, Screening of deep eutectic solvents (DESs) as Green CO2 sorbents: from solubility to viscosity, N. J. Chem. 41 (2016) 290–301, https://doi.org/10.1039/c6nj03140d.
[57] L. Zhao, J. Zhang, Intermolecular interaction of diamine-diol binary system: a mini-review, Adv. Colloid Interface Sci. 304 (2022) 102662, https://doi.org/10.1016/j.cis.2022.102662.
[58] J. Zang, W. Zhai, Y. Wang, B. Zhang, X. Ma, K. Ma, J. Zhang, Excess properties, intermolecular interaction, and CO2 capture performance of diethylene glycol monomethyl ether + ethylenediamine binary mixed solutions, J. Mol. Liq. 417 (2025) 126561, https://doi.org/10.1016/j.molliq.2024.126561.
[59] T. Aissaoui, I.M. AlNashef, Y. Benguerba, Dehydration of natural gas using choline chloride based deep eutectic solvents: COSMO-RS prediction, J. Nat. Gas. Sci. Eng. 30 (2016) 571–577, https://doi.org/10.1016/j.jngse.2016.02.007.
[60] I. Langmuir, The vapor pressure of metallic tungsten, Phys. Rev. 2 (1913) 329–342, https://doi.org/10.1103/PhysRev.2.329.

[61] K. Shahbaz, F.S. Mjalli, G. Vakili-Nezhaad, I.M. AlNashef, A. Asadov, M.M. Farid, Thermogravimetric measurement of deep eutectic solvents vapor pressure, J. Mol. Liq. 222 (2016) 61–66, https://doi.org/10.1016/j.molliq.2016.06.106.
[62] V. Majer, V. Svodoba, J. Koubek, J. Pick, Temperature dependence of heats of vaporization, saturated vapour pressures and cohesive energies for a group of amines, Collect. Czechoslov. Chem. Commun. 44 (1979).
[63] Z. Zhao, J. Gao, M. Luo, X. Liu, Y. Zhao, W. Fei, Molecular simulation and experimental study on Low-Viscosity ionic liquids for High-Efficient capturing of CO2, Energy Fuels 36 (2022) 1604–1613, https://doi.org/10.1021/acs.energyfuels.1c02928.
[64] D.R. Lide, Physical constant of inorganic compound, in: Handb. Chem. Phys., 2005: p. 474.